The Bovine Serum Albumin Coated Copper Oxide Nanoparticle for Curcumin Delivery in Biological Environment: In-vitro Drug Release

Tahmineh Atloo
University of Zanjan Faculty of Sciences
Ramin Mohammadkhani
University of Zanjan Faculty of Sciences
Ali Mohammadi
Zanjan University of Medical Sciences
Kasra Arbabi Zaboli
Zanjan University of Medical Sciences
Saeed Kaboli
Zanjan University of Medical Sciences
Hossein Rahimi
Zanjan University of Medical Sciences
Hamed Nosrati
Zanjan University of Medical Sciences
hossein danafar (✉ danafar@zums.ac.ir)
Zanjan University of Medical Sciences

Research Article

Keywords: Copper oxide, Bovine serum albumin, Curcumin

Posted Date: November 11th, 2021

DOI: https://doi.org/10.21203/rs.3.rs-1037271/v1

Abstract

In this work, first, copper oxide nanoparticles (CUO NPs) were synthesized by physical methods and then coated with the bovine serum albumin (BSA) via biologically meditated minerals to form CUO@BSA NPs. Finally, curcumin (CUR) as an anticancer drug were immobilized on the surface of CUO@BSA NPS. The properties of CUO@BSA-CUR NPS were investigated by FTIR, UV-Vis, TEM, and AFM spectroscopes. It was found that the synthesized CUO@BSA-CUR nanoparticles were spherical with a particle size of 20 to 30 nm and have a sustained release of CUR at 37°C in buffer solution. Also, the result of release in biological environment showed that maximum drug release rate for this nanocarrier in pH 7.4 was measured 75% after 48 hours. The cytotoxicity of CUO@BSA-CUR on MDA-MB-231 cell line was studied. The results showed that CUO@BSA-CUR nanoparticles have significant cytotoxic activity on this cell line, while the results of MTT assay indicated the CUO@BSA NPs have no toxicity effect on the cancer cells.

1. Introduction

Cancer is a group of diseases characterized by unregulated cell growth and the invasion and spread of cells from the original site or the original location to other parts of the body [1]. One of the most common deaths in recent decades is related to cancer, so according to the Health Organization, about 13% of deaths are due to cancer [2]. Cancer can be treated by common treatments such as surgery, chemotherapy, radiation therapy. One of the main problems in chemotherapy is the biodistribution of the chemotherapeutic compound, which can damage to normal cells [3]. To overcome these limitations, a carrier system in the form of nanoparticles must be designed that is able selectively deliver cytotoxic doses of therapeutic agents to cancer [4].

Interest in design and developing nanoparticles for applications in a wide range of various fields has continued to grow in the past decade due to their unique physical and chemical [5-8]. In particular, they have achieved significant attention mainly in biomedical fields, especially applications in biomedical fields, especially as a new method in the development of drug delivery systems [9, 10]. Nanoparticles are solid and almost spherical in shape having approximately in the 1-100 nm size range and are prepared as natural or artificial [11].

Among nanocarriers that are used in various fields of medicine and treatment, nanocrystalline semiconductors particles has been considered in drug delivery due to their unique properties such as non-toxicity, increased activity, large high surface to volume ratio, high magnetic conductivity and solubility [12]. Copper oxide as a suitable option among transition metal oxides in common form cupric oxide (CUO) possesses attractive advantage. CUO is a P-type semiconductor with a narrow energy gap and monoclinic structure. Also, CUO because of an interesting multifunctional material has applications in antimicrobials, magnetic storage media, electronics, sensors, batteries [13, 14].

Coating and modification of the surface of copper oxide nanoparticles with various biocompatible and biodegradable is important in order to obtain nanoparticles with suitable stability [15]. Bovine serum

albumin (BSA) has received much attention in drug delivery for coating nanoparticles surfaces due to its properties like biodegradability, nontoxicity, high chemical stability, easy availability and long half-life [16-19]. Albumin is the most important protein in plasma of blood, which are spherical in shape with a molecular weight of 66 kDa and ~585 amino acid [15]. Meng and its coworkers developed hybrid nanoparticles of albumin and manganese dioxide loaded with paclitaxel drug to improve chemotherapy and radiation therapy. They showed that the synthesized nanoparticles can produce the active oxygen species to improve chemotherapy and radiation therapy [20].

Curcumin (CUR) is a natural remedy and the main components of the turmeric spice, which has antioxidant, anti-inflammatory properties and is a liposoluble compound and can be easily dissolved into the organic solvent such as methanol, ethanol and acetone [21]. Also owning to the preclinical data that shows anticancer property of curcumin, it has concerned significant attention in drug delivery systems for cancer research [22-24]. In 2017, Xie and its colleagues developed nanoparticles containing the anticancer drug of curcumin for chemotherapy and photothermal therapy of cancer, as well as to protect normal cells. The results showed that the synthesized nanoparticles containing curcumin can accumulate in the tumor and also protect normal cells from the effects of radiation therapy [24].

In this study, first copper oxide nanoparticles were produced by various biophysical methods and next their surface was coated with BSA through EDC catalyst to producing strong interaction between BSA and CUO. Finally, the nano-scale carrier of CUO@BSA was utilized for loading the natural anticancer drug of curcumin which is called as CUO@BSA-CUR. The morphology and characterization of the samples were investigated by FT-IR, UV-vis, TEM, AFM techniques. Finally, the maximum release rate of the drug was evaluated by dialysis bag. The application of CUO@BSA-CUR NPs as CUR carriers was evaluated by in vitro anti-cancer activity on MDA-MB-231 cell line.

2. Material And Methods

2.1 Materials

Copper sulfate, sodium hydroxide, bovine serum albumin, 1-ethyl -3-(3-dimethylaminopropyl) carbohydratediimide (EDC), N-hydroxy succinimide (NHS), curcumin and 3- (4,5-dimethylthiazole-2-yl) -2 and 5-diphenyltetrazolium bromide (MTT) were obtained from Sigma-Aldrich (St. Louis, USA). Dimethyl sulfoxide (DMSO) was purchased from Zohr Ovi Company, Iran. . All chemicals and solvents were from general laboratory or HPLC grads, as needed, and were purchased from Emerat Chimi Company (Tehran, Iran).

2.2 Synthesis of copper oxide

First, 40 mg of copper sulfate ($CuSo_4$) was added to 6 mL of water (OH) and placed on a heater at room temperature, then 1 mL of acetic acid ($C_2H_4O_2$) was added to the solution. In the next step, 1200 mg of NaOH (sodium hydroxide) was added to the solution, and placed on the heater for 24 hours at room

temperature to turn its color to brown. Then, after 24 hours, the mixture was dialyzed to remove sodium hydroxide from the medium.

2.3 Synthesis of BSA coated CUO (CUO@BSA)

In this stage, first 10 mL of copper oxide suspension (0.8mg/ml) was combined with 32 mg of bovine serum albumin, then was stirred at room temperature for 24 hours. After 24 hours, it was washed with the centrifuge at 6,000 rpm for 15 minutes with deionized water.

2.4 Loading of curcumin on the BSA coated CUO NPs (CUO@BSA-CUR)

In order to obtain an aqueous solution of a mixture (10 mL in deionized water) of 8 mg CUO and 32 mg BSA was added and stirred for 15 min at room temperature. Then CUR solution (3 mg of CUR in 1.5 mL of ethanol) was added dropwise to above solution. The obtained solution was stirred by a magnetic stirrer for 24 h, and to purify was centrifuged for 15 min at 21,000 rpm for four cycles. In order to dry of the resulting solution, it was placed in an oven at 40 ° C for 48 h.

2.5 Characterization

2.5.1 Determine the particle size

The size and morphology of the sample of CUO@BSA-CUR NPs were characterized by transmission electron microscopy. (TEM, Cambridge 360–1990 Stereo Scan Instrument-EDS, CA)

2.5.2 FT-IR analysis

The chemical structure of the samples was determined by Fourier transform infrared spectroscopy (FT-IR). Transparent pills were prepared by mixing and grinding 2 mg of selected samples with 200 mg of white powder KBr and then compressing the resulting powder under pressure of 12 Ton. The FT-IR spectra of all samples the can record between 400 and 4,000 cm^{-1}.

2.5.3 UV-VIS analysis

Optical analysis of CUR, CUO@BSA and CUO@BSA-CUR aqueous was performed using the UV-Visible spectrum (Thermo Electronic Company Model NO Gensys 10.s) in the wavelength range of 400 to 600 nm. Every sample was diluted by 1.5 mL deionized water and kept in quarts cell.

2.5.4 AFM analysis

The surface topography of the aqueous solution of the samples was determined by atomic force microscope (AFM, Ara Research Company, Nano Expert, Model No. 0101/A, Iran). One droplet of the sample was placed on a freshly cleaved mica substrate (1 cm^2) and dried in air, AFM analysis was carried out in contact AFM mode.

2.5.5 Determine of loading efficiency

For curcumin-loading experiment, 40μL of the final sample (CUO@BSA-CUR) with the concentration (mg/mL) was dispersed in 1 mL of ethanol and then shaken in a shaker incubator (100 rpm) at 37°c for 24 h. The suspension was centrifuged for 15 minutes at 13,000 rpm. The amount of loaded CUR was determined as follows:

$$\%DL = \frac{weight\ of\ drug\ in\ nanoprticles}{wieght\ of\ nanoprticles} \times 100$$

%DL is the drug loading ratio.

2.6 Drug release study

fter immobilization of drug on nanoparticles, the release of curcumin from CUO@BSA-CUR was evaluated at PH = 7.4 using dialysis process. Briefly, 200 μL of the CUO@BSA-CUR was dispersed with 1 mL of phosphate buffer solution (PBS) then was transported to a dialysis tube with 12 kDa molecular weight cut off. The dialysis bag was immersed in 35 ml of 65% PBS solution (PBS: ethanol=65:35) .The sample was then stirred in an incubator at 37 ° C and 100 rpm. At predetermined time intervals, 1 mL of the dialysate was taken out and replaced by 1 mL new PBS. The amount of released CUR was measured using UV-visible spectroscopy at the wavelength of 428 nm. This study three times was repeated.

2.7 Cell viability test

In order to utilize the functionalized nanoparticles for biomedical applications, this study was carried out. The target cells were cultured up to a density of 80%. To do the process of cell dissociation and disperse them, trypsinization and centrifugation of the cell in the complete culture medium was carried out, and then the cells were counted with a Neubauer counting chamber. Then, the cells were seeded into a 96-well plate at a concentration of 15,000 cells per well and dissolved with 100 μL of the culture medium. The cells were kept in an incubator for 24 h in order to attach the cells to the plate surface and grow them. Then, the cells of each well were treated with the desired agents and incubated for 48 h. The cytotoxicity effect of synthesized nanoparticles was examined at various concentrations of 8, 16, 32 and 64 mg/mL. Then, after 48 h the culture medium was removed and then 20 μL of MTT with a concentration of 5 mg/mL was added to each well and incubated for 4 h. Next, after 4 h incubation 150 μL of DMSO was added to each well, and absorbance reading of each well were performed at 570 nm. Finally, the absorbance ratio of the number of surviving cells in treated samples was compared with the control group cells.

3. Results And Discussion

Characterization of CUO@BSA-CUR

3.1 FT-IR analysis

To confirm the conjugation of CUR on CUP@BSA NPs, Infrared absorption spectra of compositions of pure CUR, CUP@BSA NPs and CUR conjugated CUP@BSA NPs was performed. The results were shown in figure 1. Characteristic peaks for pure CUR were identified in the regions of 3437.76 cm^{-1} and 1628.40 cm^{-1} (C=O). The absorption peak at 3437.76 cm^{-1} can be attributed to the stretching vibrations of hydroxyl functional groups (O-H) while peak at 1628.40 cm^{-1} is due to the molecular stretching of the carboxyl group (C = O). In addition, the absorption peak 1282 cm^{-1} is related to C-O for enol structure of curcumin. FTIR spectra of CUO@BSA showed characteristic peaks at 1653.92 cm^{-1}, 3423.71 cm^{-1}, 2926.36 cm^{-1} which are assigned to the C-H aromatic bending vibrations, the stretching vibrations of O-H and CH_3, respectively. The absorption spectrum of CUO@BSA-CUR nanoparticles depicts the peaks in the region of 1653.98 cm^{-1} and 3431.72 cm^{-1} correspond to the flexural vibrations of the C-H aromatic groups and the N-H amid groups, respectively.

3.2 UV-Vis spectrophotometry analysis

UV-Vis spectroscopy was used to determine the amount of CUR conjugated on the surface of CUO@BSA NPs. Therefore, as shown in figure 2 the absorption spectrum of CUO@BSA was compared with CUO@BSA-CUR and CUR spectra. The Changes in the surface of metal nanoparticles cause a change in the absorption maximum wavelength (λ_{max}), so the binding of molecules at the surface of nanoparticles results in a shift at λ_{max} [25]. There are two peaks in 236 nm and 430 nm in CUR spectrum. In the UV-Vis spectrum of CUO@BSA, an absorption peak is observed around 260 nm. The appearance of an absorption peak at wavelengths around 415 nm in UV-Vis spectrum of CUO@BSA_CUR indicates the absorption peak for CUR conjugated to CUO@BSA compared to characteristic of CUR in the UV-Vis has a blue-shift about 15 nm at λ_{max}, which shows the binding of CUR to CUO@BSA.

3.3 Morphology of CUO @ BSA CUR nanoparticles

TEM analysis was used to determine the size and morphology of the produced nanoparticles. As shown in figure 3, TEM image of CUO@BSA-CUR NPs indicates that the nanoparticles are almost spherical in shape and have uniform morphology, and the average diameter of the as-obtained NPs was around 25 nm.

3.4 AFM analysis

One of the methods used to determine the surface topography is AFM analysis. As shown in figure 4, the morphology of CUO, CUO@BSA and CUO@BSA-CUR NPs were monitored using AFM. As obviously seen in figure 4a, the AFM height profile characterized with the Z sign shows that the thickness of CUO is almost 12 nm while the AFM analysis of BSA coated CUO exhibits that the thickness measured is the around 20 nm (see figure 5b). According to the results of AFM images in Figures 5(a, b) clearly confirms the successful binding of BSA on copper oxide nanoparticles. A noticeable geometry deformation in the figure 5c also shows that CUR has a strong affect in topography of CUO @ BSA surface. The AFM height image from CUO@BSA-CUR showed that the thickness of the final sample reached 42 nm. Thus, from the

result of AFM analysis can be concluded that CUR has been immobilized on the nanocarrier of CUO@BSA.

CUO@BSA-CUR

3.5 Investigation of drug release in neutral medium

In the design of modern delivery system, loading and controlled drug release is a very important issue, which can be depended on parameters such as pH, temperature and etc. In the present work, CUR was utilized as an anticancer drug for loading and controlled release behavior of CUO@BSA as a nanocarrier. The amount of curcumin released from the surface of NPs was measured by UV-Vis spectroscopy at the wavelength of 428 nm. As shown in figure 5, the cumulative release drug of CUR from the nanocarrier in physiological conditions (pH=7.4) was about 67% after 20 h. The release drug from CUO@BSA-CUR NPs was slower and reaches its maximum value (75%) after 48 h and can be sustained over 50 h.

3.6 Biocompatibility of nanocarrier

For drug delivery and other biomedical applications, the biocompatibility of the BSA coated CUO NPs should be investigated. Also, since nanocarriers are intentionally engineered to interact with cells, thus it is essential to study the toxicity effect of nanoparticles for biomedical and pharmaceutical applications in order to ensure that these enhancements have not any adverse effect. The cytotoxicity study of CUR, CUO@BSA NPs, and CUO@BSA-CUR NPs were carried out on MDA-MB-231 breast cancer cells. The MDA-MB-231 cells were incubated with NPs for 48 h with concentrations of 8, 16, 32, and 64 mg/mL of CUR, CUO@BSA NPs, and CUO@BSA-CUR. As shown in fig 6, the cell viability has been plotted as a function of CUR, CUO@BSA NPs, and CUO@BSA-CUR NPs at various concentrations. The results of MTT cytotoxicity test on MDA-MB-231 cells showed that by enhancing concentration, the toxicity of the free curcumin and CUO@BSA-CUR NPs increases in compared control cells, whereas CUO@BSA NPs with similar concentrations do not exhibit any toxic effect on treated cells in 48-h incubation time.

4. Conclusion

In summary, it was designed and prepared a nanocarrier based on BSA coated CUO NPs to efficiently load and delivery drug of curcumin in biomedical applications. The samples were characterized in detail the structural, colloidal by UV-Vis, FT-IR, AFM and TEM techniques, so the results demonstrated the successful synthesis of CUO@BSA-CUR NPs. The release results of anti-cancer drug curcumin within biological environment at PH = 7.4 showed that after 20 h about 67% of curcumin will release and after 48 reaches 75% which is the maximum value of release. Owing to results of the toxicity test, it was also found that BSA coating improves in vitro therapeutic outcome of CUO nanoparticles for efficient cancer treatment, so that the MTT assay exhibited no inhibitive effects of CUO@BSA NPs on cancer cells. On the other hand, CUO@BSA-CUR composite exhibited high cell-killing effect.

References

[1] Bertram, John S. “The molecular biology of cancer.” Molecular aspects of medicine, 21.6 (2000): 167-223, https://doi.org/10.1016/C2013-0-07228-3

[2] Schreiner. L. “Innovative cancer therapeutics based on polymers or biogenic drugs evaluated in murine tumor models. Dissertation, LMU München”. Diss. Lmu, Thesis, (2013), https://doi.org/10.5282/edoc.15618

[3] Rahib, Lola, et al. "Projecting cancer incidence and deaths to 2030: the unexpected burden of thyroid, liver, and pancreas cancers in the United States." *Cancer research* 74.11 (2014): 2913-2921.

[4] Manjili. H. K, Malvandi. H, Mousavi M-S and Danafar. H, "Preparation and physicochemical characterization of biodegradable mPEGPCL coreshell micelles for delivery of artemisinin ". Pharm Sci. 22(4) (2016); 234–243.

[5] Nomani, Alireza, et al. "Preparation and characterization of copolymeric polymersomes for protein delivery." Drug research 67(8) (2017): 458-465.

[6] Molavi, Hossein, et al. "Evaluation of UiO-66 metal organic framework as an effective sorbent for Curcumin's overdose." Applied Organometallic Chemistry 32(4) (2018): e4221.

[7] Danafar, H. "Applications of copolymeric nanoparticles in drug delivery systems." Drug research 66(10) (2016): 506-519.

[8] Danafar, Hossein. "Study of the composition of polycaprolactone/poly (ethylene glycol)/polycaprolactone copolymer and drug-to-polymer ratio on drug loading efficiency of curcumin to nanoparticles." Jundishapur Journal of Natural Pharmaceutical Products 12(1) (2017).

[9] Nosrati, Hamed, et al. "Methotrexate-conjugated L-lysine coated iron oxide magnetic nanoparticles for inhibition of MCF-7 breast cancer cells." *Drug development and industrial pharmacy* 44(6) (2018): 886-894.

[10] Nosrati, Hamed, et al. "Enzymatic stimuli-responsive methotrexate-conjugated magnetic nanoparticles for target delivery to breast cancer cells and release study in lysosomal condition." *Journal of Biomedical Materials Research Part A* 106(6) (2018): 1646-1654.

[11] Xu, Tao, Ning Zhang, Heather L. Nichols, Donglu Shi, Xuejun Wen. "Modification of nanostructured materials for biomedical applications." Materials Science and Engineering: C 27(3) (2007): 579-594.

[12] Wang, Hui, et al. "Preparation of CuO nanoparticles by microwave irradiation." Journal of crystal growth 244.1 (2002): 88-94.

[13] Kose. S., et al. "Some physical properties of In doped copper oxide films produced by ultrasonic spray pyrolysis." *Current Applied Physics* 12.3 (2012): 890-895.

[14] Applerot, Guy, et al. "Understanding the antibacterial mechanism of CuO nanoparticles: revealing the route of induced oxidative stress." *Small* 8.21 (2012): 3326-3337.

[15] Nosrati, Hamed, et al. "Preparation of magnetic albumin nanoparticles via a simple and one-pot desolvation and co-precipitation method for medical and pharmaceutical applications." International journal of biological macromolecules 108 (2018): 909-915.

[16] Nosrati, Hamed, et al. "Bovine Serum Albumin (BSA) coated iron oxide magnetic nanoparticles as biocompatible carriers for curcumin-anticancer drug." *Bioorganic chemistry* 76 (2018): 501-509.

[17] Kratz, Felix. "Albumin as a drug carrier: design of prodrugs, drug conjugates and nanoparticles." *Journal of controlled release* 132.3 (2008): 171-183.

[18] Ranucci, Elisabetta, et al. "Modification of albumins by grafting poly (amido amine) chains." *Polymer* 36.15 (1995): 2989-2994.

[19] Wongsasulak, Saowakon, et al. "The effect of solution properties on the morphology of ultrafine electrospun egg albumen–PEO composite fibers." *Polymer* 48.2 (2007): 448-457.

[20] Meng, Lingtong, et al. "Facile deposition of manganese dioxide to albumin-bound paclitaxel nanoparticles for modulation of hypoxic tumor microenvironment to improve chemoradiation therapy." Molecular pharmaceutics 15.2 (2018): 447-457.

[21] R. Wilken. R, Veena. M.S, Wang. M.B, Srivatsan. E.S, "Curcumin: a review of anti-cancer properties and therapeutic activity in head and neck squamous cell carcinoma", Mol. Canc. 10 (1) (2011) 12.

[22] Charmi J, et al. "Polyethylene glycol (PEG) decorated graphene oxide nanosheets for controlled release curcumin delivery." Heliyon 5 (2019): 01466.

[23] Abbasi R, et al. " Synthesis and characterization of PEGylated iron and graphene oxide magnetic composite for curcumin delivery." Appl Organomet Chem 34(10) (2020): 1-9

[24] Xie, Jiani, et al. "Therapeutic nanoparticles based on curcumin and bamboo charcoal nanoparticles for chemo-photothermal synergistic treatment of cancer and radioprotection of normal cells." *ACS applied materials & interfaces* 9.16 (2017): 14281-14291.

[25] Aziz, Shujahadeen B., et al. "Investigation of metallic silver nanoparticles through UV-Vis and optical micrograph techniques." Int. J. Electrochem. Sci 12 (2017): 363-373.

Figures

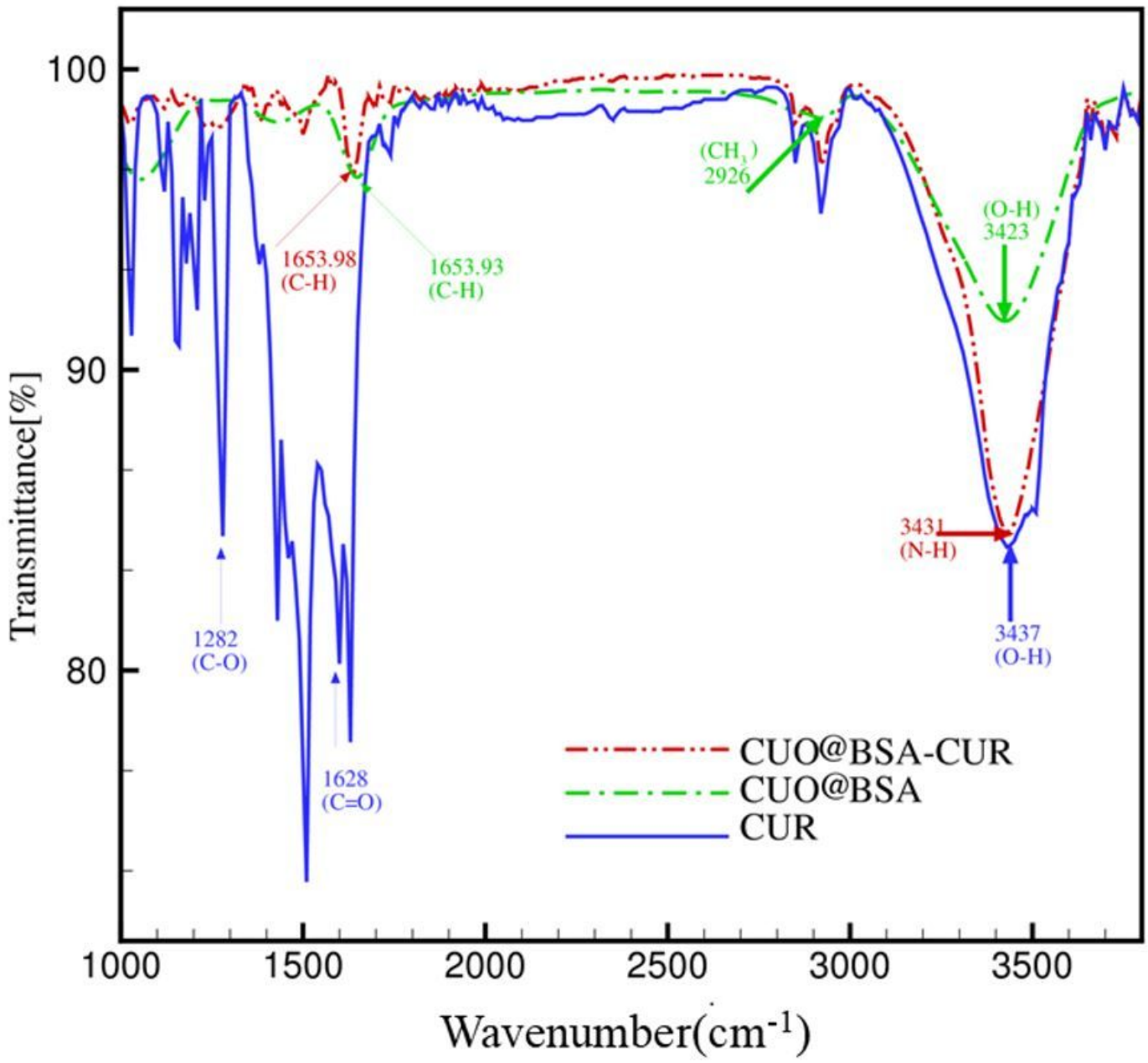

Figure 1

FT-IR spectra of CUR, CUO@BSA and CUO@BSA-CUR.

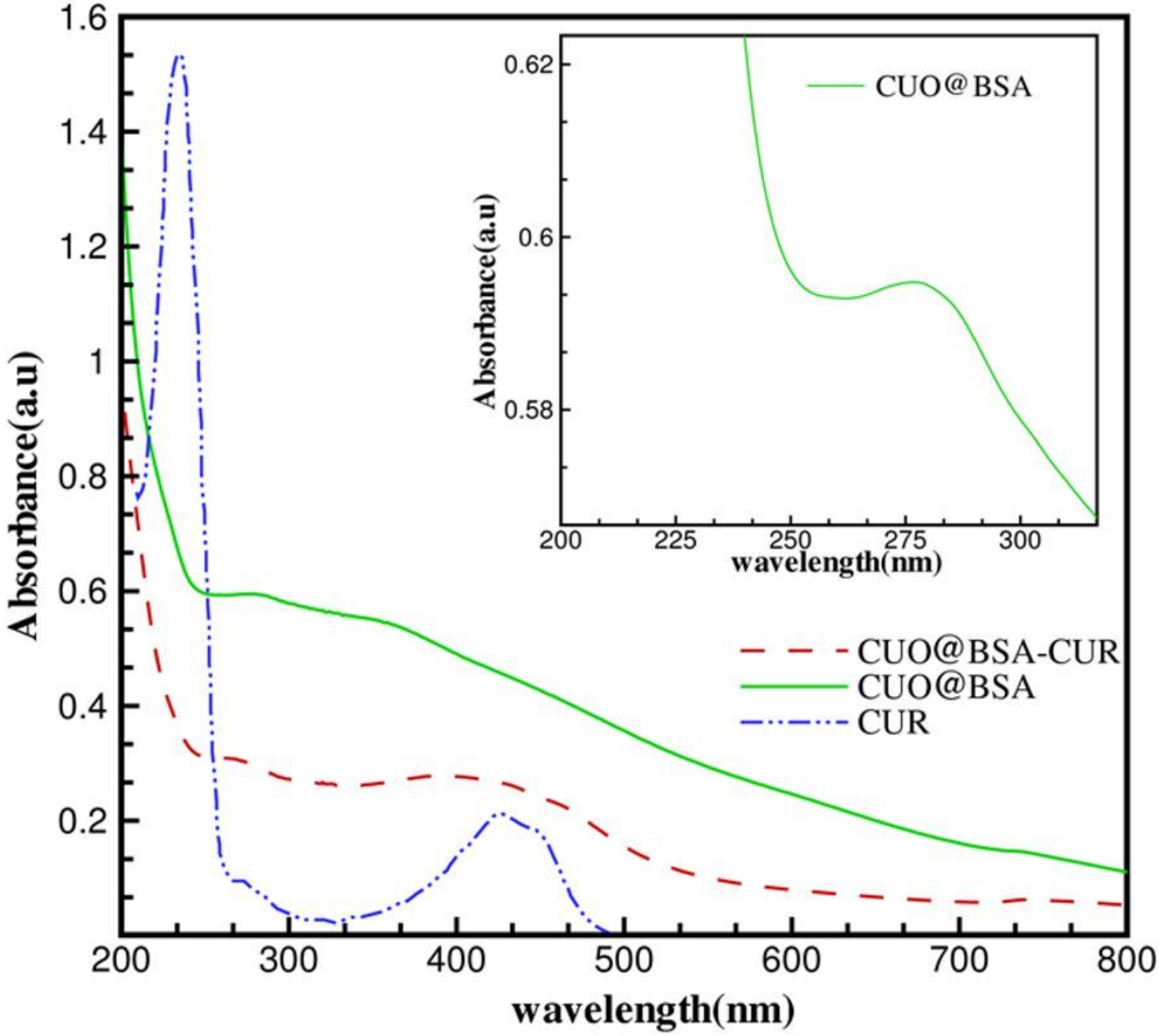

Figure 2

UV-Vis absorption spectrum of CUR, CUO@BSA and CUO@BSA-CUR. Inset shows UV-Vis spectrum of CUO@BSA around the absorption peak.

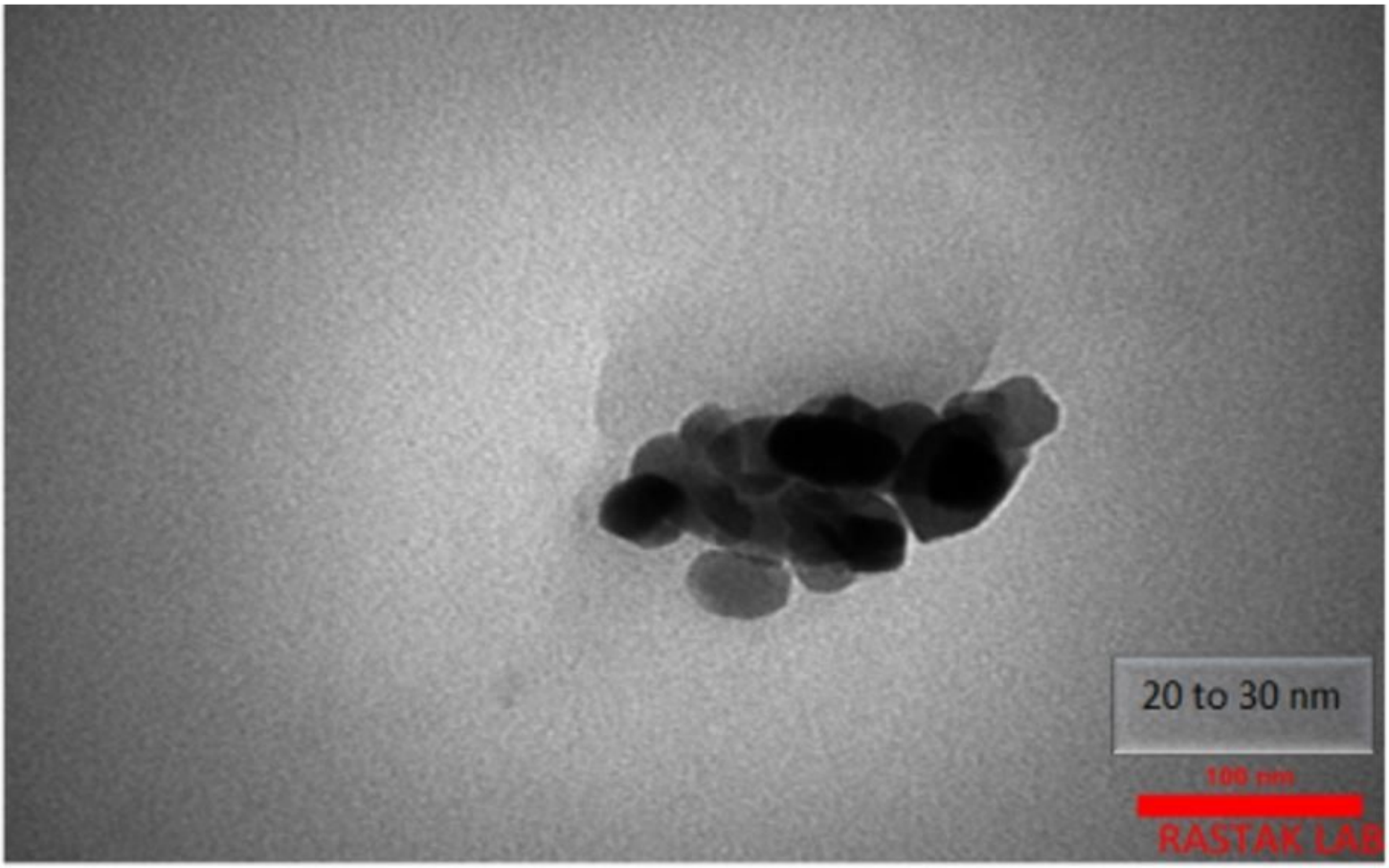

Figure 3

TEM images of CUR conjugated on CUO@BSA.

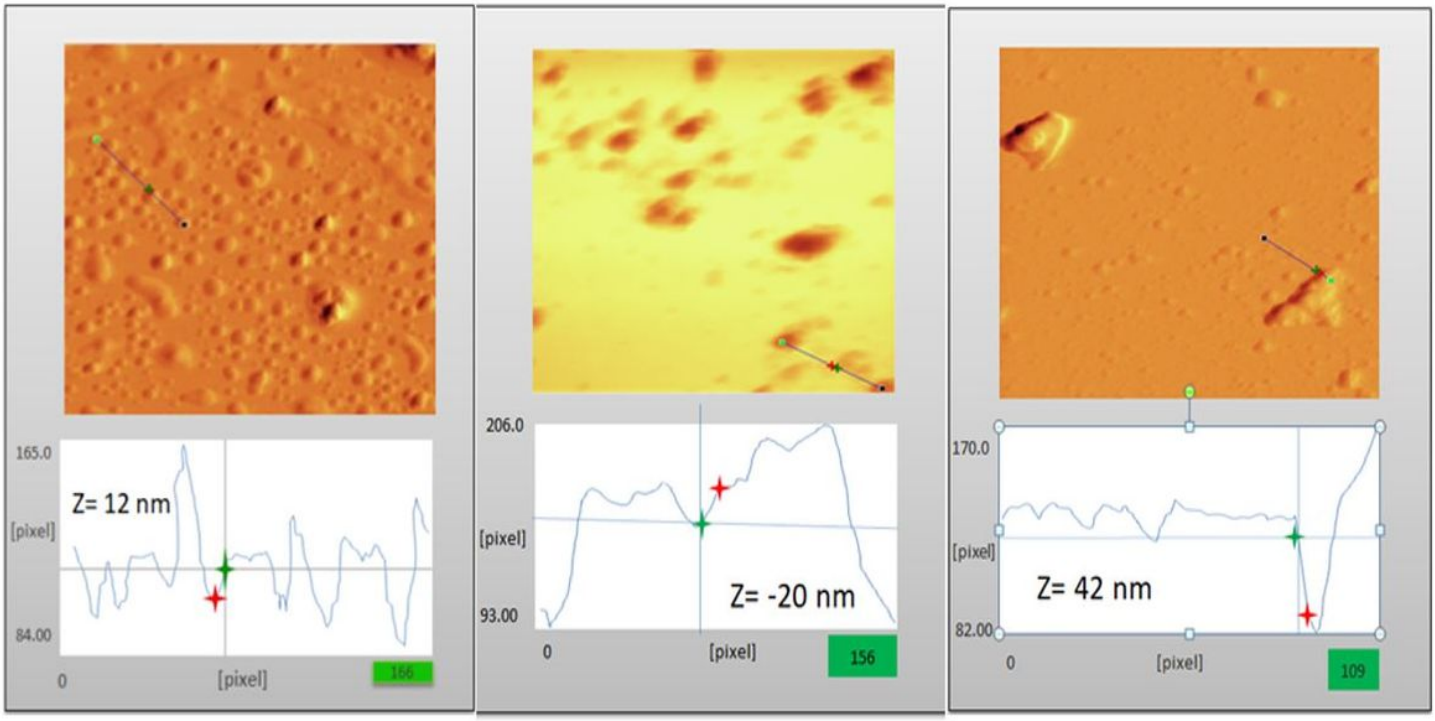

Figure 4

Topography by atomic force microscope (AFM) for (a) CUR (b) CUO @BSA (c) CUO@BSA-CUR

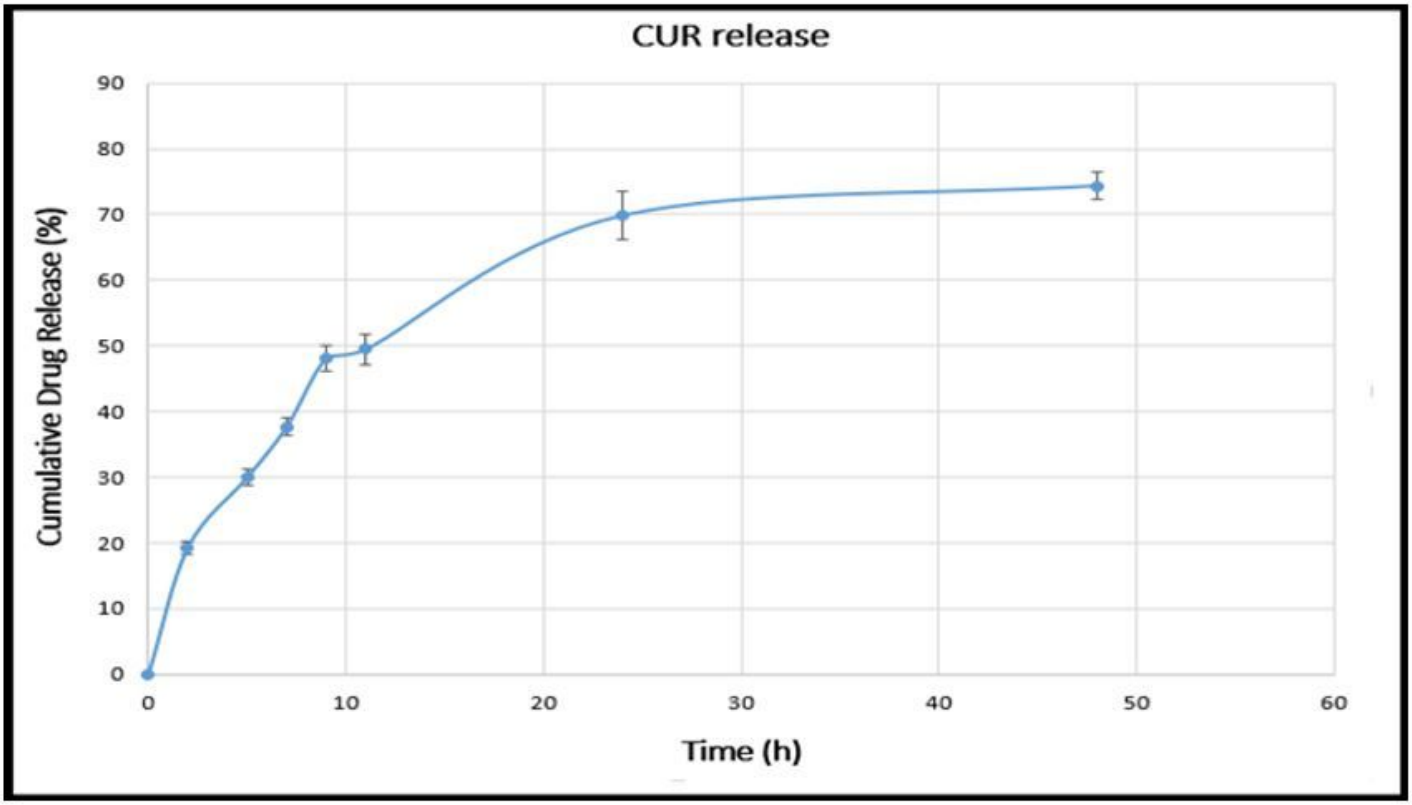

Figure 5

The release profiles of the CUR from NPs at pH of 7.4

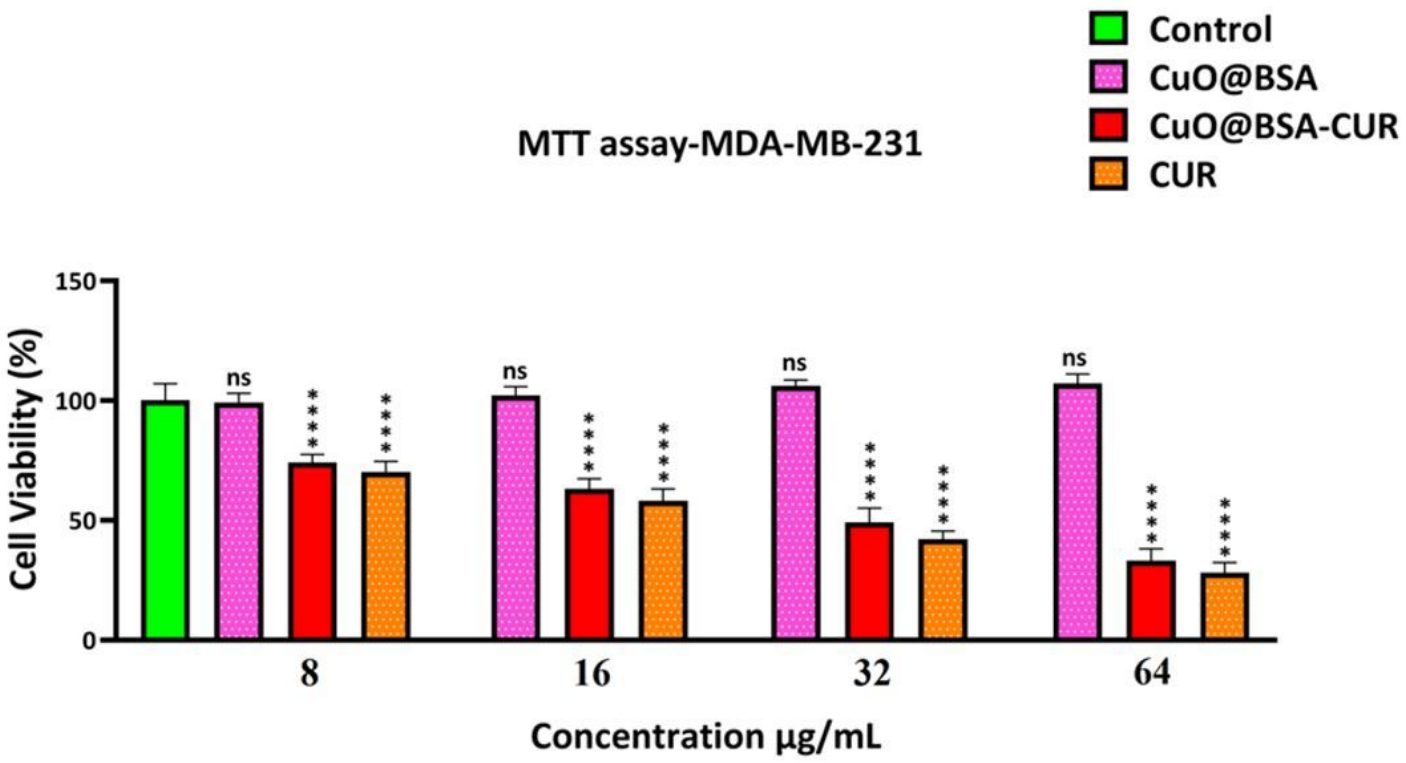

Figure 6

Cytotoxicity analysis of free CUR, CUO@BSA, and CUO@BSA-CUR after incubation 48 h on cancer cells at pH = 7.4.